Gradual disintegration of the floral symmetry gene network is implicated in the evolution of a wind-pollination syndrome

Jill C. Preston[1], Ciera C. Martinez[2], and Lena C. Hileman

Department of Ecology and Evolutionary Biology, University of Kansas, Lawrence, KS 66045

Edited by Enrico Sandro Coen, John Innes Centre, Norwich, United Kingdom, and approved January 3, 2011 (received for review July 30, 2010)

Angiosperms exhibit staggering diversity in floral form, and evolution of floral morphology is often correlated with changes in pollination syndrome. The showy, bilaterally symmetrical flowers of the model species *Antirrhinum majus* (Plantaginaceae) are highly specialized for bee pollination. In *A. majus*, *CYCLOIDEA* (*CYC*), *DICHOTOMA* (*DICH*), *RADIALIS* (*RAD*), and *DIVARICATA* (*DIV*) specify the development of floral bilateral symmetry. However, it is unclear to what extent evolution of these genes has resulted in flower morphological divergence among closely related members of Plantaginaceae differing in pollination syndrome. We compared floral symmetry genes from insect-pollinated *Digitalis purpurea*, which has bilaterally symmetrical flowers, with those from closely related *Aragoa abietina* and wind-pollinated *Plantago major*, both of which have radially symmetrical flowers. We demonstrate that *Plantago*, but not *Aragoa*, species have lost a dorsally expressed *CYC*-like gene and downstream targets *RAD* and *DIV*. Furthermore, the single *P. major CYC*-like gene is expressed across all regions of the flower, similar to expression of its ortholog in closely related *Veronica serpyllifolia*. We propose that changes in the expression of duplicated *CYC*-like genes led to the evolution of radial flower symmetry in *Aragoa*/*Plantago*, and that further disintegration of the symmetry gene pathway resulted in the wind-pollination syndrome of *Plantago*. This model underscores the potential importance of gene loss in the evolution of ecologically important traits.

Evolution of flower symmetry is tightly correlated with pollinator shifts and has been proposed as a key innovation within the angiosperms (1–6). In the plantain family (Plantaginaceae, Lamiales), morphological and phylogenetic analyses suggest that the ancestral flower was five-parted, bilaterally symmetrical (monosymmetrical and zygomorphic), and insect-pollinated (7, 8). For example, in *Antirrhinum majus* (snapdragon, Antirrhineae) and *Digitalis purpurea* (foxglove, Digitalideae), large bee-pollinated flowers are five-parted and establish bilateral symmetry due to differential growth rates along the dorsiventral axis. The dorsal (adaxial), lateral, and ventral (abaxial) petals and stamens are easily distinguishable based on differences in shape and/or ornamentation, further reinforcing a single plane of symmetry within mature flowers (Fig. 1; Fig. S1) (8–13).

Veroniceae is the sister tribe to Digitalideae, and includes the large cosmopolitan genera *Veronica* (*ca.* 450 species) and *Plantago* (*ca.* 200 species) and the small páramo endemic genus *Aragoa* (19 species), each of which is monophyletic based on phylogenetic analyses (14–19). In contrast to the ancestral flower form found in Digitalideae, several Veroniceae species have flowers that are four-parted, radially symmetrical (polysymmetrical and actinomorphic), and/or wind-pollinated (Fig. 1) (8, 15, 20–22). The small flowers of *Veronica* are primarily fly- and/or self-pollinated, and develop four sepals and four petals (23, 24). The enlarged dorsal petal is inferred to develop from two dorsal petals that fuse early in development (11, 25) and, consequently, *Veronica* flowers have retained bilateral symmetry within the petal whorl (11, 25). Whereas the radially symmetrical showy flowers of *Aragoa* have retained the ancestral number of five sepals but have four identical petals and stamens (11, 12, 21), the diminutive radially symmetrical flowers of wind-pollinated *Plantago* are four-merous in all three outer organ whorls (Fig. 1). In early development, both *Aragoa* and *Plantago* flowers are bilaterally symmetrical due to the unidirectional emergence of organs in a ventral-to-dorsal sequence (21). However, flowers at mid to late stages of development in both genera are fully radially symmetrical (21, 26).

It is hypothesized that changes in the expression or biochemical function of genes that establish the ancestral condition of floral bilateral symmetry underlie the evolution of radial symmetry in the *Aragoa*/*Plantago* clade (8, 21, 27). The floral symmetry genetic pathway is best understood in *A. majus*, and involves the action of three dorsal identity genes, *CYCLOIDEA* (*CYC*), *DICHOTOMA* (*DICH*), and *RADIALIS* (*RAD*), and one ventral identity gene, *DIVARICATA* (*DIV*) (13, 28–32). *CYC* and *DICH* are recently duplicated type II TCP transcription factors that establish bilateral symmetry in both early and late flower development, partly through their positive regulation of the MYB transcription factor *RAD* in the dorsal petals and staminode (13, 29, 31, 33). Although not expressed outside the dorsal petals and staminode, RAD appears to negatively regulate the ventral identity protein DIV in the dorsal and lateral regions of the flower (29, 30). Thus, ventral identity is confined to the ventral region of the flower (28, 30).

Unlike close relatives *Veronica serpyllifolia* and *D. purpurea*, which have two and three *CYC*-like genes, respectively, only one *CYC*-like gene has been recovered from *Plantago lanceolata* (ribwort plantain; subgenus *Psyllium sensu lato*) and *P. major* (common plantain; subgenus *Plantago*) genomes, suggesting a recent gene loss event in the *Plantago* lineage (14, 18, 27, 33–35). Furthermore, Reardon et al. recently demonstrated that expression of this gene does not appear to be confined to the dorsal region of the *P. lanceolata* flower (27). Instead, evidence suggests expression in the region below the flower, correlating with the loss of differentiated dorsal flower identity and a shift to radial symmetry. Interestingly, a nondorsal pattern of expression for the *V. serpyllifolia* ortholog to the single *Plantago CYC*-like gene was also recently demonstrated (34). The aim of this study is to better understand the role of floral symmetry gene network evolution in the shift from bilateral to radial symmetry in the Veroniceae. Here we test three nonexclusive hypotheses: (*i*) loss of a dorsally expressed *CYC*-like paralog predates evolution of radial symmetry in the *Aragoa*/*Plantago* lineage; (*ii*) the nondorsal expression pattern of the single *Plantago CYC*-like gene

Author contributions: J.C.P. and L.C.H. designed research; J.C.P. and C.C.M. performed research; J.C.P. analyzed data; and J.C.P. and L.C.H. wrote the paper.

The authors declare no conflict of interest.

This article is a PNAS Direct Submission.

Data deposition: The sequences reported in this paper have been deposited in the GenBank database (accession nos. HQ853598–HQ853667.

[1]To whom correspondence should be addressed. E-mail: jcpxt8@ku.edu.

[2]Present address: Section of Plant Biology, University of California, Davis, CA 95616.

This article contains supporting information online at www.pnas.org/lookup/suppl/doi:10.1073/pnas.1011361108/-/DCSupplemental.

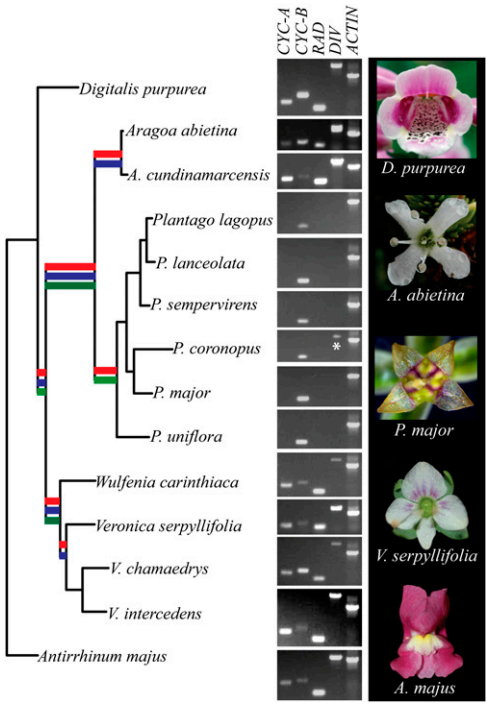

Fig. 1. Maximum-likelihood phylogram based on combined nuclear markers showing evolution of flower symmetry and its underlying genetic pathway in Plantaginaceae. Bold branches indicate supported (>70% bootstrap and/or >90% posterior probability) generic relationships based on the chloroplast markers *rps2*, *rbcL*, *ndhF*, *rps16*, and *matK-trnK* (blue branch) (7, 15, 20), combined nuclear markers *DEL*, ITS, and *DIV* intron (red branch), and *ACT* (green branch). Morphological transitions include a reduction from five large (*Antirrhinum* and *Digitalis*) to four small (*Veronica*, *Plantago*, and *Aragoa*) petals, and a shift from bilateral (*Antirrhinum*, *Digitalis*, and *Veronica*) to radial flower symmetry (*Aragoa* and *Plantago*). PCR analyses using conserved primers on genomic DNA demonstrate that the loss of showy petals, but not radial flower symmetry, is correlated with a loss of the A-clade *CYC*-like gene and its downstream targets *RAD* and *DIV* in six *Plantago* species, representing four of the five monophyletic subgenera (21). Note: Our sequence analysis confirmed that the band amplified by the *DIV* primers in *P. coronopus* (indicated with an asterisk) is the *DIV*-like paralog *PcDVL* (Fig. 2*C*).

evolved before the loss of its sister paralog; and (*iii*) the loss of a dorsally expressed *CYC*-like paralog resulted in loss, or change in expression, of its downstream targets.

Results

***Plantago* and *Aragoa* Are More Closely Related to *Veronica* than to *Digitalis*.** Although the sister relationship of *Aragoa* and *Plantago* is well-supported based on multiple markers (7, 15, 20) (Fig. 1), previous phylogenetic analyses have been equivocal regarding the relationship between the monophyletic genera *Aragoa*/*Plantago*, *Veronica*, and *Digitalis* (7, 14–20). Analyses based on combined *rbcL*, *ndhF*, and *rps2*, as well as *trnL-F* chloroplast sequences, support a close relationship between *Aragoa*/*Plantago* and *Veronica*, with *Digitalis* sister to these genera together (7, 15, 20) (Fig. 1). However, analyses based on the *matK-trnK* and *rps16* introns and the internal transcribed spacer (ITS) give different topologies with varying levels of support (20).

To better resolve these relationships with the ultimate aim of elucidating the direction of evolutionary change within the floral symmetry gene network, we combined ITS sequences generated from multiple studies (15, 18, 20, 36) and generated partial sequences of the nuclear *DELILA* (*DEL*) and *ACTIN* (*ACT*) genes and the full *DIV* intron for *A. majus*, *D. purpurea*, two *Aragoa* species, six *Plantago* species representing four of the five monophyletic subgenera (except the *DIV* intron), three *Veronica* species representing three of the twelve subgenera, and the *Veronica* outgroup *Wulfenia carinthiaca* (14–19) (Fig. 1; Fig. S2). *DEL*, *ACT*, and the *DIV* intron have been successfully used to resolve species relationships in eukaryotes and other plant groups (37–39).

With the exception of *ACT*, individual analyses of aligned nucleotides strongly supported the monophyly of *Veronica*, *Plantago*, and *Aragoa*, as previously suggested (14–19) (Fig. S2). Furthermore, consistent with combined analyses based on chloroplast gene markers (7, 20), all trees from individual analyses resolved a sister relationship between *Aragoa*/*Plantago* and *Wulfenia*/*Veronica* genes, with the genes from *D. purpurea* being more distantly related (Fig. S2). Results were concordant between maximum-likelihood and Bayesian reconstructions, and were supported by likelihood bootstrap (LB) and/or posterior probability (PP) values >70% and >90%, respectively (Fig. S2). Based on concordance between gene trees, *DEL*, ITS, and *DIV* intron sequences were concatenated for further analysis. The best trees based on combined analyses were not significantly different from independent analyses; the monophyly of each genus and the sister relationship between *Aragoa*/*Plantago* and *Wulfenia*/*Veronica* was supported by LB (100% and 76%, respectively) and/or PP (100% and 86%, respectively) values (Fig. 1; Fig. S2).

Floral Symmetry Gene Degeneration in Representative Species of *Plantago* but Not *Aragoa*. To determine copy-number and orthology/paralogy relationships among floral symmetry genes, multiple clones derived from PCR using various *CYC*-, *RAD*-, and *DIV*-like primer sets were sequenced from *D. purpurea*, *V. serpyllifolia*, *P. major*, *P. lanceolata*, and *A. abietina*. Consistent with previous studies, only one *CYC*-like gene was isolated from *P. major* (*PmTCP1*) and *P. lanceolata* (*PlTCP1*), three were isolated from *D. purpurea* (*DpCYC1*, *DpCYC2*, and *DpCYC3*), and two were isolated from *V. serpyllifolia* (*VsCYC1* and *VsCYC2*) (14, 27, 33–35). Similar to *V. serpyllifolia*, two putatively functional *CYC*-like genes were also isolated from *A. abietina* (*AaCYC1* and *AaCYC2*).

Phylogenetic analyses of these sequences, supplemented with sequences from additional species (see below), revealed a well-supported (LB of 100%, PP of 100%) sister relationship between *DpCYC1*, *VsCYC1*, and *AaCYC1* ("A" clade in Fig. 2*A*) and among the recently duplicated *D. purpurea* genes *DpCYC2* and *DpCYC3*, *VsCYC2*, *AaCYC2*, *PmTCP1*, and *PlTCP1* ("B" clade in Fig. 2*A*; LB of 80%, PP of 100%). Although inferred gene relationships within the A and B clades did not completely track the species phylogeny (Fig. 1 versus Fig. 2*A*), there was limited support from the *CYC* dataset for generic relationships within either the A or B clade. Thus, together with support for the species tree topology, the *CYC*-like gene tree suggests a single gene duplication event at the base of Digitalideae + Veroniceae, followed by A lineage gene loss at the base of *Plantago*. Comparison of maximum-likelihood models found no evidence of positive or relaxed selection on branches leading to *AaCYC1*, *AaCYC2*/*PmTCP1*/*PlTCP1*, or *PmTCP1*/*PlTCP1* (Table S1).

Sequencing of multiple clones, in combination with phylogenetic analyses, revealed single *RAD* and *DIV* gene orthologs in *A. majus*, *D. purpurea*, *V. serpyllifolia*, and *A. abietina* (Fig. 2 *B* and *C*). Again, comparison of maximum-likelihood models found no evidence of positive or relaxed selection on branches leading to the *A. abietina* genes (Table S1). By contrast, despite the isolation of more distantly related paralogs in *Plantago* (*PmRAD4* and *PlDIVL*; Fig. 2 *B* and *C*), no *RAD* or *DIV* gene orthologs were found in inflorescence cDNA pools of *P. major* or *P. lanceolata* (Fig. 2 *B* and *C*).

To further verify that the genomes of all *Plantago* species lack A-clade *CYC*, *RAD*, and *DIV* orthologs, and to test whether symmetry gene copy number is consistent across genera, highly

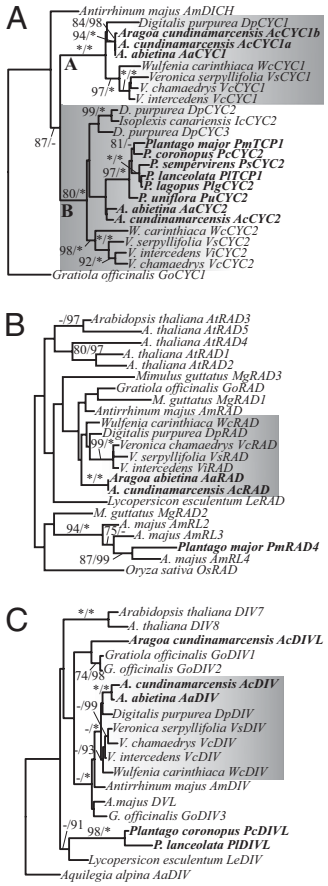

Fig. 2. Maximum-likelihood phylograms showing best estimates of floral symmetry gene relationships. (*A*) *CYC*-like genes were duplicated following the divergence of Antirrhineae (represented by *Antirrhinum majus*) and Digitalideae (represented by *Digitalis purpurea*) + Veroniceae (represented by *Wulfenia*, *Veronica*, *Aragoa*, and *Plantago*), giving rise to two gene clades designated A and B (shaded). *Plantago* species have a single B-clade *CYC*-like gene (bold), but no genes were found within the *CYC* A clade, suggesting loss of this gene at the base of *Plantago*. (*B*) *Plantago* genomes have *RAD*-like paralogs (bold) but lack *RAD* orthologs. (*C*) *Plantago* genomes have *DIV*-like (*DIVL*) paralogs (bold) but lack *DIV* orthologs. Maximum-likelihood bootstrap values >70% (*Left*) and Bayesian posterior probabilities >90% (*Right*) are shown. Asterisks denote support values of 100%.

conserved *CYC*, *RAD*, and *DIV* primers were designed (Table S2). These primers amplified A-clade *CYC* and B-clade *CYC*, *RAD*, and *DIV* fragments from genomic DNA of *A. majus*, *D. purpurea*, *W. carinthiaca*, and *Veronica* and *Aragoa* species (Figs. 1 and 2; Fig. S2). However, only B-clade *CYC* genes were amplified from genomic DNA of representative *Plantago* species (Figs. 1 and 2; Fig. S2), confirming the loss of A-clade *CYC*, *RAD*, and *DIV* before the diversification of *Plantago*.

***PmTCP1* Expression Is Not Restricted to the Dorsal Domain.** To test predictions that *CYC*-like and *RAD*-like genes are expressed dorsally throughout *D. purpurea*, but not *P. major*, flower development, quantitative (q)RT-PCR and in situ hybridization were carried out (Figs. 3 and 4). Unfortunately, because *Aragoa* is endemic to the páramo of Colombia and Venezuela, similar material was not available for determining gene expression patterns in this genus.

Quantitative RT-PCR analyses on dissected *D. purpurea* flowers revealed that the transcript levels for all three *CYC*-like genes, and the single *RAD*-like gene, were at least 62-fold higher in dorsal petals than in lateral petals, ventral petals, stamens, and

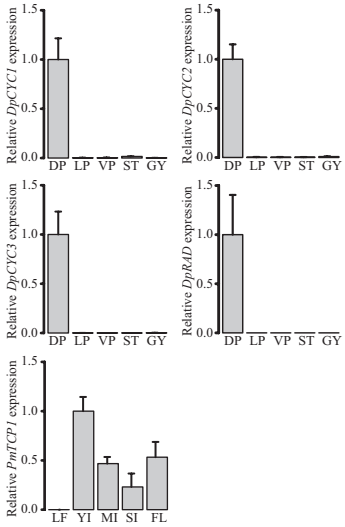

Fig. 3. Quantitative RT-PCR analyses showing relative symmetry gene expression levels in different tissues of *Digitalis purpurea* and *Plantago major*. Expression levels are relative to *EF1alpha* (*D. purpurea*) or *UBQ-5* (*P. major*), with SDs for four technical replicates. DP, dorsal petals; FL, flowers from proximal half of the SI (see below) inflorescence; GY, gynoecia; LF, leaf; LP, lateral petals; MI, midstage (11 mm long) inflorescence; SI, proximal half of young inflorescence with flowers partially removed; ST, stamens; VP, ventral petal; YI, young (7 mm long) inflorescence.

gynoecia (Fig. 3). Thus, unlike the B-clade *V. serpyllifolia* ortholog *VsCYC2*, which is expressed across dorsal, lateral, and ventral petals (34), petal expression of the B-clade genes *DpCYC2* and *DpCYC3* was characteristic of *CYC*-like genes from other species with bilaterally symmetrical flowers (13, 34, 40–48).

For in situ hybridization in *D. purpurea*, one recent duplicate in the B clade (*DpCYC3*), *DpCYC1*, and *DpRAD* were selected for further analysis (Fig. 2 *A* and *B*). Similar to qRT-PCR analyses, mRNA of all three genes was most strongly detectable in the dorsal region of the floral meristem and in later-stage flowers (Fig. 4 *A*–*H*). At later stages of flower development, during petal fusion, all three genes were expressed most strongly in the dorsal petals, with a lower level of expression in stamens, gynoecia, and lateroventral petals for the *CYC*-like genes (Fig. 4 *B*, *E*, and *H*). Staining was undetectable on sections hybridized with sense control probes for each gene.

Flowers of *P. major* cannot be easily dissected due to their small size. Instead, cDNA from differently staged inflorescences and vegetative tissues was prepared for qRT-PCR. *PmTCP1* expression was highest in inflorescence tissues, with no detectable expression in leaves (Fig. 3). Within inflorescence tissues, *PmTCP1* expression was over 1.5-fold higher in young (7 mm) versus midstage (11 mm) whole inflorescences. Furthermore, expression was over 2-fold higher in flowers separated from the proximal half of a young inflorescence compared with the proximal half of the same young inflorescence with most of its flowers removed (Fig. 3).

Similar to the qRT-PCR data, in situ hybridization revealed expression of *PmTCP1* in *P. major* inflorescences (Fig. 4 *I* and *J*). In early development, *PmTCP1* was expressed throughout floral meristems, and in mid- to late-stage development, *PmTCP1* expression was evident in all organs of the flower, in the dorsal, lateral, and ventral domains (Fig. 4 *I* and *J*). Expression throughout the flowers was similar to that of *Histone4*, a marker of cell proliferation (Fig. 4*L*), and appeared to be specific, based on the lack of staining in sections probed with a sense control (Fig. 4*K*). The wide expression pattern of *PmTCP1* across the flower was similar to that previously found for its *V. serpyllifolia* ortholog, *VsCYC2*, but

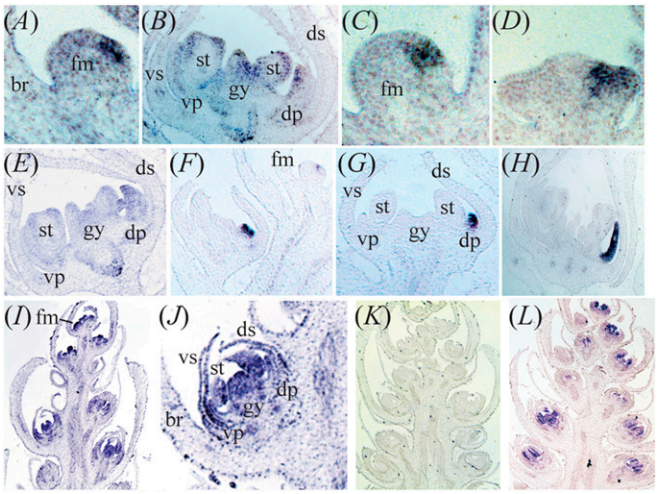

Fig. 4. In situ hybridization analyses showing spatiotemporal patterns of symmetry genes in *Digitalis purpurea* and *Plantago major*. *DpCYC1* (*A* and *B*), *DpCYC3* (*C–E*), and *DpRAD* (*F–H*) are expressed asymmetrically in floral meristems and flowers, whereas *PmTCP1* (*I* and *J*) is expressed symmetrically in floral meristems and flowers. (*K*) No staining is detectable in *P. major* inflorescences probed with the *PmTCP1* sense probe. (*L*) *PmHistone4* is strongly expressed in actively dividing cells of *P. major* flowers. br, bract; dp, dorsal petal; ds, dorsal sepal; fm, floral meristem; gy, gynoecium; st, stamen; vp, ventral petal; vs, ventral sepal.

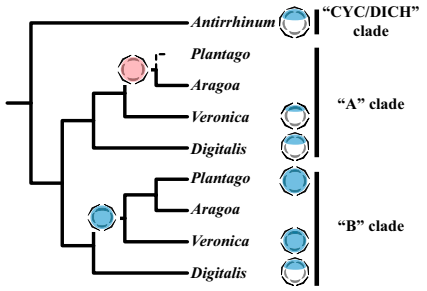

Fig. 5. Hypothesis of floral symmetry evolution based on phylogenetic analyses and expression of *CYC*-, *RAD*-, and *DIV*-like genes. The ancestral *CYC*-like gene at the base of tribes Antirrhineae, Digitalideae, and Veroniceae was probably expressed asymmetrically on the dorsal side of the floral meristem and flower. The ancestral *CYC*-like gene was maintained through speciation events and duplicated independently at the base of the Antirrhineae (represented by *Antirrhinum*), and in the ancestor of Digitalideae + Veroniceae (represented by *Digitalis*, *Veronica*, *Aragoa*, and *Plantago*). At the base of Veroniceae, regulatory evolution occurred within the B clade, from dorsally restricted expression to expression across the flower; expression data from *Veronica* suggest that the *Veronica* B-clade *CYC* gene product no longer regulates *RAD* expression (34). Because both *Aragoa* and *Plantago* flowers are radially symmetrical and there is no evidence of relaxed selection on *AaCYC1* (or on *AaRAD* or *AaDIV*), it is hypothesized that there was an expansion of the A-clade *CYC*-like gene in the ancestor of these genera (shaded flower on branch). In the *Plantago* lineage, the A-clade *CYC*-like gene is lost (dotted line). Loss of the A-clade *CYC*-like gene coincides with loss of downstream genes *RAD* and *DIV*, and with the evolutionary change from a showy to a nonpigmented, diminutive corolla, and from insect to wind pollination. Expression patterns illustrated in blue are based on empirical data (13, 31, 34); patterns illustrated in red are hypothesized as described above.

different from the dorsal expression patterns of orthologs *DpCYC2* and *DpCYC3* and that reported for *P. lanceolata* (27, 34).

Discussion

Our findings support the hypothesis that radially symmetrical flowers in the *Aragoa*/*Plantago* lineage evolved gradually through gene duplication, expression diversification, and degeneration in the symmetry developmental genetic pathway (21, 27, 34, 35) (this study) (Fig. 5). Specifically, we have shown that at least two species of *Aragoa* have maintained apparently functional copies of both dorsal (*CYC* and *RAD*) and ventral (*DIV*) identity genes, which may be important for the development of its attractive corolla (Fig. 1). By contrast, degeneration of both the dorsal and ventral identity programs in six representative species of *Plantago* implicates the lateral floral organ identity program in the development of all four diminutive petals (Fig. 1), the proposed default pathway in *A. majus* (13, 31). Given all available evidence, we hypothesize a single origin of floral radial symmetry in the ancestor of *Aragoa*/*Plantago* due to the expansion of gene expression in the *CYC*-like A and B clades, followed by further disintegration of the symmetry gene pathway, including the loss of a dorsally expressed A-clade *CYC* paralog, as well as *RAD* and *DIV* orthologs, resulting in the wind-pollination syndrome of *Plantago* species (Fig. 5).

Gradual disintegration of the floral symmetry pathway in the *Aragoa*/*Plantago* lineage is supported by two lines of evidence: phylogenetic and gene expression. Phylogenetic analyses strongly support a *CYC*-like gene duplication event at the base of the tribes Digitalideae + Veroniceae, followed by a more recent duplication event within Digitalideae (27, 33, 35) (this study). Both paralogs generated from the first duplication event were maintained in *D. purpurea*, *W. carinthiaca*, and numerous species of *Veronica* and *Aragoa*. However, independent studies demonstrate the loss of the A-clade *CYC* gene along the lineage leading to *Plantago*, represented by distantly related *P. major*, *P. coronopus*, *P. uniflora*, *P. lanceolata*, *P. lagopus*, and *P. sempervirens* (27, 35) (this study) (dotted line in Fig. 5).

Gene expression analyses of A-clade *CYC* genes from *D. purpurea* and *V. serpyllifolia*, B-clade *CYC* genes from *D. purpurea*, and *CYC* and *DICH* from *A. majus* suggest that the ancestral Digitalideae + Veroniceae *CYC*-like gene was expressed dorsally within the flower (13, 31, 34) (this study) (Fig. 5). This is similar to expression patterns of other *CYC*-like genes within the Lamiales and, in combination with the observed dorsal coexpression of *DpRAD* and *VsRAD*, is consistent with an ancestral function in dorsal petal identity specification (13, 31, 34, 40, 44–46). By contrast, expression of *V. serpyllifolia* and *P. major* B-clade *CYC*-like genes is not restricted to the dorsal domain of the flower (34) (this study), and our data suggest that this condition is derived relative to dorsally restricted expression of closely related *CYC*-like genes. Both *VsCYC2* and *PmTCP1* are expressed ubiquitously across floral meristems and petals; expression varies within the stamen whorl. These data demonstrate an expansion of the B-clade *CYC*-like gene expression domain within Veroniceae, suggesting a loss (nonfunctionalization) or change (neofunctionalization) of developmental function following gene duplication (Fig. 5). Our working hypothesis is that the Veroniceae B-clade *CYC*-like gene has acquired a novel developmental function in regulating flower size, correlating with a significant reduction of flower size in this lineage.

Codon models suggest that the *A. abietina* floral symmetry genes are functionally constrained, implicating expression changes in the evolution of floral radial symmetry. Based on evidence from *VsCYC2* and *PmTCP1*, we infer that *AaCYC2* is also expressed throughout the flower (34) (this study). Furthermore, given that *AaRAD* and *AaDIV* appear to be functionally constrained, we predict a similar expansion in expression of the A-clade *CYC*-like gene in the ancestor of *Aragoa* and *Plantago*, resulting in a single origin of floral radial symmetry. Assuming that this most parsimonious interpretation is correct, we suggest two ways in which *AaRAD* and *AaDIV* might have been maintained in the genus

Aragoa. One scenario is that AaRAD no longer negatively regulates *AaDIV*, and therefore all four symmetry genes contribute to development of the entire corolla whorl. Alternatively, *AaRAD* and *AaDIV* may have evolved novel functions in flower development. Regardless of which hypothesis is correct, our results are similar to those from previous studies showing expansion or contraction of *CYC*-like gene expression correlated with independent shifts from bilateral to radial symmetry in the showy corollas of *Cadia purpurea* (Leguminoseae), *Bournea leiophylla* (Gesneriaceae), and disk flowers of *Gerbera hybrida* (40, 42, 49).

The final step in the transition from insect to wind pollination in the *Plantago* genus was likely due to the loss of the A-clade *CYC*-like gene (Fig. 5) and the correlated loss of *RAD* and *DIV*. In *A. majus*, *RAD* expression is positively regulated by CYC in the dorsal region of the flower. In turn, RAD negatively regulates the DIV protein in the dorsal and lateral regions of the flower, leading to differential petal and stamen identity along the dorsiventral axis of the flower (28–30, 50). Unlike *A. majus*, there is no intrawhorl organ differentiation in *Plantago* flowers (21). Assuming that our search for *RAD* and *DIV* orthologs was exhaustive, the absence of these genes from representative *Plantago* genomes indicates the loss of both the dorsal and ventral identity programs. This would implicate the same "lateral" (*sensu A. majus*) identity program in the development of dorsal, lateral, and ventral floral organs of *Plantago*, highlighting the potential importance of gene duplication and loss in the evolution of form.

Materials and Methods

Plant Material. Seeds of *Digitalis purpurea* ("Candy Mountain") and *Veronica serpyllifolia* were obtained from Thompson and Morgan Seed; seeds of *Plantago major* were obtained from the University of Washington Medicinal Herb Garden. Plants were grown in the greenhouse under standard long-day (16 h light/8 h dark) conditions. Fresh material of *P. lanceolata* was collected from wild populations in Lawrence, KS. DNA of *Aragoa abietina* (reference no. 12226), *A. cundinamarcensis* (reference no. 11177), *P. coronopus* (reference no. 2763), *P. lagopus* (reference no. 9433), *P. sempervirens* (reference no. 9426), *P.* (formerly *Littorella*) *uniflora* (reference no. 2798), *V. chamaedrys* (reference no. 7419), *V. intercedens* (reference no. 9211), and *W. carinthiaca* (reference no. 8940) was obtained from Kew Gardens DNA Bank.

Isolation of Nuclear Markers. *DEL*, *ACT*, and the *DIV* intron were amplified from genomic DNA using the primers MYCF1/R2, ACT1/2, and DIV-55-F/403-R, respectively, based on their phylogenetic utility in other plant groups (34, 37–39) (Table S2). Although *ACT* genes are multicopy in angiosperms, ACT1/2 selectively amplified genes belonging to the REP clade, with closest homology to the *Solanum tuberosum* (potato, Solanaceae) genes *Ac46*, *Ac71*, and *Ac75* (51). PCR bands were individually gel-extracted (Qiagen) and cloned into the pGEM-T vector (Invitrogen). At least four clones were sampled per PCR band for sequencing on both strands.

Floral Symmetry Gene Isolation. Multiple *CYC*-like clones were sequenced from inflorescence cDNA synthesized from total mRNA or genomic DNA, following amplification with a set of degenerate forward primers (CYCF1, CYC73aaF, CYC73aF, and CYC73bF) in combination with the reverse primers CYC-R2 and/or poly-TQT (34, 52). These primers have been used previously to successfully amplify *CYC*-like genes from across Plantaginaceae (34, 52). To isolate *RAD* and *DIV* orthologs, the degenerate forward primers RAD.deg.F, RAD.deg (2).F, DIV.deg.F, and DIV.deg (2).F were used in combination with the reverse primer poly-TQT, and multiple clones were sequenced as previously described (Table S2) (34). To verify the presence/absence of *CYC*, *RAD*, and *DIV* genes, conserved primers were designed based on aligned *A. majus* and *V. serpyllifolia* sequences. The primer pairs Arag.CYC.A.F/R, Arag.CYC.B.F/R, RAD-70-F/240-R, and DIV-55-F/403-R were used to amplify *CYC* A, *CYC* B, *RAD*, and *DIV* orthologs, respectively, from genomic DNA (Table S2).

Phylogenetic Analysis. *DEL*, *ACT*, ITS, and floral symmetry genes were separately aligned using MAFFT, with readjustment by eye in MacClade (53–55). Phylogenetic relationships were estimated using maximum-likelihood methods in GARLI 0.951 and Bayesian methods in MrBayes 3.1.2 (56, 57). For both types of analysis, MrModeltest 2.3 was used to estimate the best model of molecular evolution (GTR + I + Γ for the *DIV* intron, *ACT*, and ITS; HKY + I + Γ for *CYC*, *DIV*, and *DEL*; SYM I + Γ for *RAD*) (58). Maximum-likelihood analyses were run using 10 random addition sequences, and Bayesian analyses were run twice for 1 million generations, sampling every 1,000 generations. LB values were obtained using 200 replicates in GARLI. Combined analyses were partitioned in GARLI-Part-0.97 and MrBayes based on different model selection by MrModeltest.

Tests for Selection. To test for positive or relaxed selection along specific branches of the symmetry gene trees, maximum-likelihood branch (one- and two-ratio) and branch-site (M1a, Null, and model A) models were run on an alignment of the longest sequences from *A. majus*, *D. purpurea*, *V. serpyllifolia*, *P. major*, *P. lanceolata*, and *A. abietina* using the codeml program in PAML Version 4.3 (59). Foreground branches were specified as those ancestral to clades containing *AaCYC1* only, *PmTCP1*, *PlTCP1*, and *AaCYC2* together, *PmTCP1* and *PlTCP1* together, *AaRAD* only, and *AaDIV* only. Nested models were compared against a χ^2 distribution of trees using a likelihood ratio test. To test for elevated ω (synonymous-to-nonsynonymous site ratio) on the foreground branch(es), the one- and two-ratio models were compared (60). To incorporate heterogeneity of parameters over both sites and branches, M1a was compared with model A and, when significant at the 0.05 level, null model A was compared with model A (61).

Quantitative RT-PCR. Total RNA was extracted from vegetative tissues and dissected floral tissues of *D. purpurea* and *P. major* using TriReagent (Ambion) according to the manufacturer's instructions. Extracted RNA was treated with rDNaseI (Ambion), and cDNA was synthesized using an iScript cDNA synthesis kit (Bio-Rad). Quantitative RT-PCR was carried out as previously described (62). The gene-specific primers pairs DpCYC1qrtF/R, DpCYC2qrtF/R, DpCYC3qrtF/R, PmTCP1qrtF/R, and DpRADqrtF/R were designed in Primer3 (63) (Table S2). *EF1alpha* and *UBQ-5* showed little transcriptional variation across different tissues, and were therefore selected as the reference genes. Cycle threshold values were corrected for transcriptional stability and normalized against *EF1alpha* (*D. purpurea*) or *UBQ-5* (*P. major*). For each gene, the mean and SD were determined for four technical replicates.

In Situ Hybridization. Inflorescences of *D. purpurea* and *P. major* were fixed in formaldehyde-acetic acid-alcohol (FAA), dehydrated in an alcohol series, and embedded in paraffin wax blocks. Antisense and sense gene-specific probes of *DpCYC1*, *DpCYC3*, *DpRAD*, and *PmTCP1* spanning the C-terminal end of the coding regions and the 3′-UTRs were generated using T7 and T3 RNA Taq polymerase (Roche) according to the manufacturer's instructions. As an experimental control, an antisense probe was generated for *PmHistone4* as described previously (34). In situ hybridization was performed as in refs. 64 and 65.

ACKNOWLEDGMENTS. We thank Felipe Zapata for help with phylogenetic analyses and two anonymous reviewers for comments on an early version of the manuscript. DNA material was used with the permission of the Board of Trustees of the Royal Botanic Gardens, Kew. C.C.M. was supported by National Institute of General Medical Science Grant 5R25GM078441 through the Post-Baccalaureate Research Education Program at the University of Kansas. This work was supported by National Science Foundation Grant IOS-0616025 (to L.C.H.).

1. Donoghue MJ, Ree RH, Baum DA (1998) Phylogeny and the evolution of flower symmetry in the Asteridae. *Trends Plant Sci* 3:311–317.
2. Endress PK (1999) Symmetry in flowers: Diversity and evolution. *Int J Plant Sci* 160 (Suppl 6):S3–S23.
3. Knapp S (2010) On 'various contrivances': Pollination, phylogeny and flower form in the Solanaceae. *Philos Trans R Soc Lond B Biol Sci* 365:449–460.
4. Ree RH, Donoghue MJ (1999) Inferring rates of change in flower symmetry in asterid angiosperms. *Syst Biol* 48:633–641.
5. Sargent RD (2004) Floral symmetry affects speciation rates in angiosperms. *Proc Biol Sci* 271:603–608.
6. Vamosi JC, Vamosi SM (2010) Key innovations within a geographical context in flowering plants: Towards resolving Darwin's abominable mystery. *Ecol Lett* 13: 1270–1279.
7. Olmstead RG, et al. (2001) Disintegration of the Scrophulariaceae. *Am J Bot* 88: 348–361.
8. Reeves PA, Olmstead RG (1998) Evolution of novel morphological and reproductive traits in a clade containing *Antirrhinum majus* (Scrophulariaceae). *Am J Bot* 85: 1047–1056.
9. Arber A (1932) Studies on flower structure. I. On a peloria of *Digitalis purpurea* L. *Ann Bot* 46:929–939.

10. Coen ES, et al. (1995) Evolution of floral symmetry. *Philos Trans R Soc Lond B Biol Sci* 350:35–38.
11. Endress PK (2001) Evolution of floral symmetry. *Curr Opin Plant Biol* 4:86–91.
12. Kampny CM, Dengler NG (1997) Evolution of flower shape in Veroniceae (Scrophulariaceae). *Plant Syst Evol* 205:1–25.
13. Luo D, Carpenter R, Vincent C, Copsey L, Coen E (1996) Origin of floral asymmetry in *Antirrhinum*. *Nature* 383:794–799.
14. Albach DC, Meudt HM (2010) Phylogeny of *Veronica* in the Southern and Northern Hemispheres based on plastid, nuclear ribosomal and nuclear low-copy DNA. *Mol Phylogenet Evol* 54:457–471.
15. Bello MA, Chase MW, Olmstead RG, Ronsted N, Albach D (2002) The páramo endemic *Aragoa* is the sister genus of *Plantago* (Plantaginaceae; Lamiales): Evidence from plastid *rbcL* and nuclear ribosomal ITS sequence data. *Kew Bull* 57:585–597.
16. Cho Y, Mower JP, Qiu Y-L, Palmer JD (2004) Mitochondrial substitution rates are extraordinarily elevated and variable in a genus of flowering plants. *Proc Natl Acad Sci USA* 101:17741–17746.
17. Rahn K (1996) A phylogenetic study of Plantaginaceae. *Bot J Linn Soc* 120:145–198.
18. Ronsted N, Chase MW, Albach DC, Bello MA (2002) Phylogenetic relationships within *Plantago* (Plantaginaceae): Evidence from nuclear ribosomal ITS and plastid *trnL-F* sequence data. *Bot J Linn Soc* 139:323–338.
19. Tay ML, Meudt HM, Garnock-Jones PJ, Ritchie PA (2010) DNA sequences from three genomes reveal multiple long-distance dispersals and non-monophyly of sections in Australasian *Plantago* (Plantaginaceae). *Aust J Bot* 23:47–68.
20. Albach DC, Meudt HM, Oxelman B (2005) Piecing together the "new" Plantaginaceae. *Am J Bot* 92:297–315.
21. Bello MA, Rudall PJ, González F, Fernández-Alonso JL (2004) Floral morphology and development in *Aragoa* (Plantaginaceae) and related members of the order Lamiales. *Int J Plant Sci* 165:723–738.
22. Oxelman B, Backlund M, Bremer B (1999) Relationships of the Buddlejaceae s. l. investigated using parsimony jackknife and branch support analysis of chloroplast *ndh*F and *rbc*L sequence data. *Syst Bot* 24:164–182.
23. Grime JP, Hodgson JG, Hunt R (1988) *Comparative Plant Ecology* (Unwin Hyman, London).
24. Pennell FW (1935) *The Scrophulariaceae of Eastern Temperate North America* (Acad Nat Sci, Philadelphia) Monograph 1.
25. Kampny CM, Dickinson TA, Dengler NG (1993) Quantitative comparison of floral development in *Veronica chamaedrys* and *Veronicastrum virginicum* (Scrophulariaceae). *Am J Bot* 80:449–460.
26. Hong D-Y (1984) Taxonomy and evolution of the Veroniceae (Scrophulariaceae) with special reference to palynology. *Opera Bot* 75:1–60.
27. Reardon W, Fitzpatrick DA, Fares MA, Nugent JM (2009) Evolution of flower shape in *Plantago lanceolata*. *Plant Mol Biol* 71:241–250.
28. Almeida J, Rocheta M, Galego L (1997) Genetic control of flower shape in *Antirrhinum majus*. *Development* 124:1387–1392.
29. Corley SB, Carpenter R, Copsey L, Coen E (2005) Floral asymmetry involves an interplay between TCP and MYB transcription factors in *Antirrhinum*. *Proc Natl Acad Sci USA* 102:5068–5073.
30. Galego L, Almeida J (2002) Role of *DIVARICATA* in the control of dorsoventral asymmetry in *Antirrhinum* flowers. *Genes Dev* 16:880–891.
31. Luo D, et al. (1999) Control of organ asymmetry in flowers of *Antirrhinum*. *Cell* 99: 367–376.
32. Preston JC, Hileman LC (2009) Developmental genetics of floral symmetry evolution. *Trends Plant Sci* 14:147–154.
33. Hileman LC, Baum DA (2003) Why do paralogs persist? Molecular evolution of *CYCLOIDEA* and related floral symmetry genes in Antirrhineae (Veronicaceae). *Mol Biol Evol* 20:591–600.
34. Preston JC, Kost MA, Hileman LC (2009) Conservation and diversification of the symmetry developmental program among close relatives of snapdragon with divergent floral morphologies. *New Phytol* 182:751–762.
35. Reeves PA, Olmstead RG (2003) Evolution of the TCP gene family in Asteridae: Cladistic and network approaches to understanding regulatory gene family diversification and its impact on morphological evolution. *Mol Biol Evol* 20:1997–2009.
36. Albach DC, Chase MW (2001) Paraphyly of Veronica (Veroniceae; Scrophulariaceae): Evidence from the internal transcribed spacer (ITS) sequences of nuclear ribosomal DNA. *J Plant Res* 114:9–18.
37. Fan C, Purugganan MD, Thomas DT, Wiegmann BM, Xiang JQ (2004) Heterogeneous evolution of the *myc*-like anthocyanin regulatory gene and its phylogenetic utility in *Cornus* L. (Cornaceae). *Mol Phylogenet Evol* 33:580–594.
38. Howarth DG, Donoghue MJ (2009) Duplications and expression of *DIVARICATA*-like genes in Dipsacales. *Mol Biol Evol* 26:1245–1258.
39. Keeling PJ (2001) Foraminifera and Cercozoa are related in actin phylogeny: Two orphans find a home? *Mol Biol Evol* 18:1551–1557.
40. Broholm SK, et al. (2008) A TCP domain transcription factor controls flower type specification along the radial axis of the *Gerbera* (Asteraceae) inflorescence. *Proc Natl Acad Sci USA* 105:9117–9122.
41. Busch A, Zachgo S (2007) Control of corolla monosymmetry in the Brassicaceae *Iberis amara*. *Proc Natl Acad Sci USA* 104:16714–16719.
42. Citerne HL, Pennington RT, Cronk QCB (2006) An apparent reversal in floral symmetry in the legume *Cadia* is a homeotic transformation. *Proc Natl Acad Sci USA* 103: 12017–12020.
43. Feng X, et al. (2006) Control of petal shape and floral zygomorphy in *Lotus japonicus*. *Proc Natl Acad Sci USA* 103:4970–4975.
44. Gao Q, Tao JH, Yan D, Wang YZ, Li ZY (2008) Expression differentiation of *CYC*-like floral symmetry genes correlated with their protein sequence divergence in *Chirita heterotricha* (Gesneriaceae). *Dev Genes Evol* 218:341–351.
45. Hileman LC, Kramer EM, Baum DA (2003) Differential regulation of symmetry genes and the evolution of floral morphologies. *Proc Natl Acad Sci USA* 100:12814–12819.
46. Song CF, Lin QB, Liang RH, Wang YZ (2009) Expressions of ECE-CYC2 clade genes relating to abortion of both dorsal and ventral stamens in *Opithandra* (Gesneriaceae). *BMC Evol Biol* 9:244.
47. Wang Z, et al. (2008) Genetic control of floral zygomorphy in pea (*Pisum sativum* L.). *Proc Natl Acad Sci USA* 105:10414–10419.
48. Zhang W, Kramer EM, Davis CC (2010) Floral symmetry genes and the origin and maintenance of zygomorphy in a plant-pollinator mutualism. *Proc Natl Acad Sci USA* 107:6388–6393.
49. Zhou X-R, Wang Y-Z, Smith JF, Chen R (2008) Altered expression patterns of TCP and MYB genes relating to the floral developmental transition from initial zygomorphy to actinomorphy in *Bournea* (Gesneriaceae). *New Phytol* 178:532–543.
50. Costa MMR, Fox S, Hanna AI, Baxter C, Coen E (2005) Evolution of regulatory interactions controlling floral asymmetry. *Development* 132:5093–5101.
51. An SS, Möpps B, Weber K, Bhattacharya D (1999) The origin and evolution of green algal and plant actins. *Mol Biol Evol* 16:275–285.
52. Howarth DG, Donoghue MJ (2005) Duplications in *CYC*-like genes from Dipsacales correlate with floral form. *Int J Plant Sci* 166:357–370.
53. Katoh T, Toh H (2008) Recent developments in the MAFFT multiple sequence alignment program. *Brief Bioinform* 9:286–298.
54. Katoh K, Misawa K, Kuma K, Miyata T (2002) MAFFT: A novel method for rapid multiple sequence alignment based on fast Fourier transform. *Nucleic Acids Res* 30: 3059–3066.
55. Maddison DR, Maddison WP (2003) *MacClade 4: Analysis of Phylogeny and Character Evolution* (Sinauer, Sunderland, MA), Version 4.0.6.
56. Ronquist F, Huelsenbeck JP (2003) MrBayes 3: Bayesian phylogenetic inference under mixed models. *Bioinformatics* 19:1572–1574.
57. Zwickl D (2006) Genetic algorithm approaches for the phylogenetic analysis of large biological sequence datasets under the maximum likelihood criterion. PhD thesis (University of Texas at Austin, Austin, TX).
58. Nylander JAA (2004) MrModeltest (Evolutionary Biology Centre, Uppsala University, Uppsala, Sweden), Version 2.
59. Yang Z (2007) PAML 4: Phylogenetic analysis by maximum likelihood. *Mol Biol Evol* 24:1586–1591.
60. Yang Z (1998) Likelihood ratio tests for detecting positive selection and application to primate lysozyme evolution. *Mol Biol Evol* 15:568–573.
61. Zhang J, Nielsen R, Yang Z (2005) Evaluation of an improved branch-site likelihood method for detecting positive selection at the molecular level. *Mol Biol Evol* 22: 2472–2479.
62. Preston JC, Hileman LC (2010) SQUAMOSA-PROMOTER BINDING PROTEIN 1 initiates flowering in *Antirrhinum majus* through the activation of meristem identity genes. *Plant J* 62:704–712.
63. Rozen S, Skaletsky HJ (2000) Primer3 on the WWW for general users and for biologist programmers. *Bioinformatics Methods and Protocols: Methods in Molecular Biology*, eds Krawetz S, Misener S (Humana, Totowa, NJ), pp 365–386.
64. Jackson D (1991) In situ hybridization in plants. *Molecular Plant Pathology: A Practical Approach*, eds Bowles DJ, Gurr SJ, McPherson M (Oxford Univ Press, Oxford), pp 163–174.
65. Preston JC, Kellogg EA (2007) Conservation and divergence of *APETALA1*/*FRUITFULL*-like gene function in grasses: Evidence from gene expression analyses. *Plant J* 52: 69–81.